Title
BENZENE AND CARBON MONOXIDE ADSORBED ON Pt(lll): A LEED INTENSITY ANALYSIS

Authors
Ogletree, D.F.
Hove, M.A. Van
Somorjai, G.A.

Publication Date
1986-07-01

LBL-21502
Preprint

Lawrence Berkeley Laboratory
UNIVERSITY OF CALIFORNIA

Materials & Chemical Sciences Division

Submitted to Surface Science

BENZENE AND CARBON MONOXIDE ADSORBED ON Pt (111): A LEED INTENSITY ANALYSIS

D.F. Ogletree, M.A. Van Hove, and G.A. Somorjai

July 1986

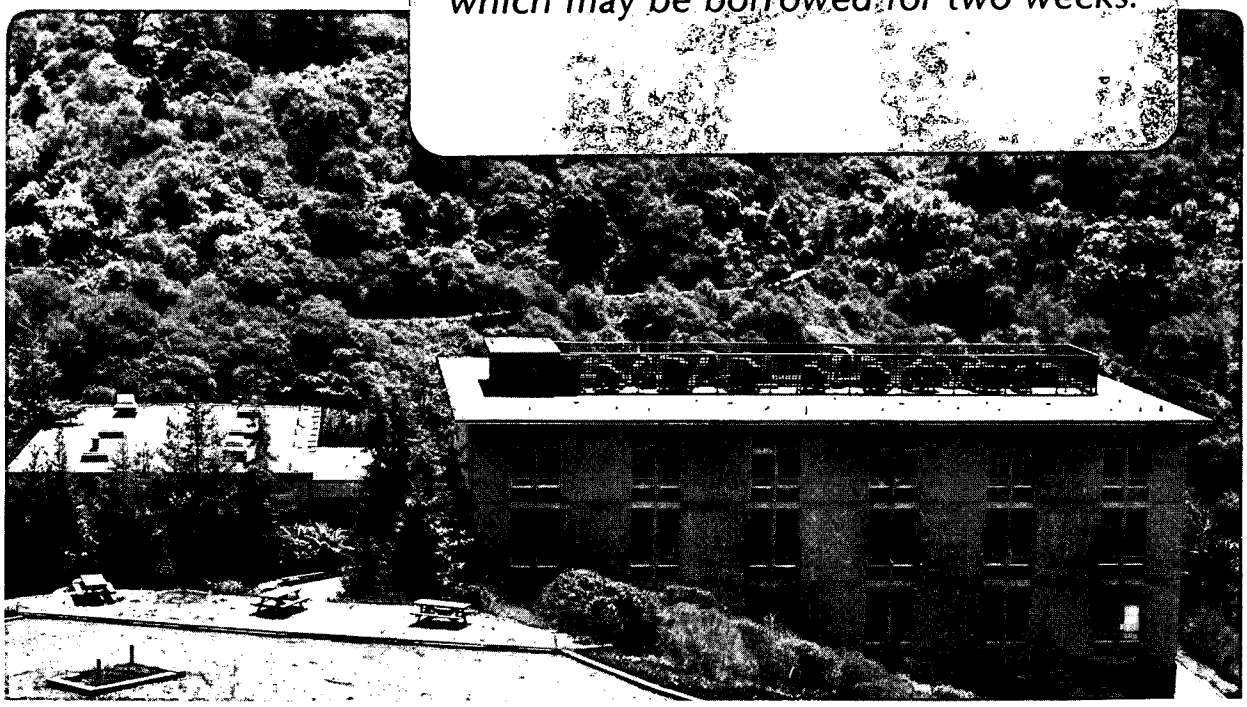

Prepared for the U.S. Department of Energy under Contract DE-AC03-76SF00098

DISCLAIMER

LBL-21502

BENZENE AND CARBON MONOXIDE ADSORBED ON Pt(111): A LEED INTENSITY ANALYSIS

D.F. Ogletree, M.A. Van Hove, and G.A. Somorjai

Materials and Chemical Sciences Division
Lawrence Berkeley Laboratory and
Department of Chemistry
University of California, Berkeley
Berkeley, California 94720
USA

ABSTRACT

The structure of the Pt(111)-(2√3x4)rect-2C_6H_6+4CO coadsorption system has been analyzed with dynamical calculations of low-energy electron diffraction intensities. The benzene molecules are oriented with their carbon rings parallel to the surface, centered over bridge sites with local C_{2v} symmetry. A large carbon ring expansion is found, with possible differences in C-C bond lengths within the same ring. The carbon ring is planar within ~0.05Å. There are probably two carbon monoxide molecules for each benzene molecule within the unit cell. Their likely locations are also bridge sites.

1. INTRODUCTION

We have recently performed Low-energy electron diffraction (LEED) intensity analyses to study two different ordered structures of benzene coadsorbed with carbon monoxide on the (111) face of rhodium.[1,2] In this report we present a similar study of an ordered structure of benzene coadsorbed with carbon monoxide on the (111) face of platinum.

The change of metal substrate results in significant changes in the adsorption site and in the distortions of the carbon ring for the benzene molecule. These differences in benzene-metal bonding may be related to the different chemistry of benzene over platinum and rhodium catalysts.

Two ordered structures of benzene on Pt(111) were observed a number of years ago.[3] The unit cells of these two structures can be labeled $(\begin{smallmatrix}4 & 4\\ \bar{2} & 2\end{smallmatrix})$ or (2√3x4)rect for the first structure and $(\begin{smallmatrix}5 & 5\\ \bar{2} & 2\end{smallmatrix})$ or (2√3x5)rect for the second structure (two equivalent notations are being used here to relate the surface superlattice to the substrate surface lattice, the matrix notation and a modified, "rectangular", Wood notation).

Benzene chemisorbs as intact molecules on the Pt(111) surface. Thermal desorption spectroscopy (TDS) studies using hydrogenated and deuterated benzene show that no significant hydrogen exchange occurs between adsorbed benzene molecules or between adsorbed benzene and coadsorbed atomic hydrogen below 400 K, and also that adsorbed (labeled) benzene can be displaced

intact from the surface by further exposure to benzene.[4] Above 400 K molecular desorption and decomposition are competing processes.

Vibrational spectroscopy studies also indicate that benzene is chemisorbed intact on Pt(111), and with the benzene ring parallel to the surface. High resolution electron energy loss spectroscopy (HREELS) data were interpreted in terms of flat lying benzene molecules in high-symmetry sites.[5] Results of near-edge x-ray adsorption fine structure spectroscopy (NEXAFS) also support intact benzene molecules π-bonded parallel to the Pt(111) surface.[6]

A more recent HREELS study has demonstrated that the ordered LEED patterns observed for benzene on Pt(111) are due to coadsorbed carbon monoxide.[7] Different carbon monoxide to benzene ratios give rise to the (2$\sqrt{3}$x4)rect and (2$\sqrt{3}$x5)rect LEED patterns, while in the absence of carbon monoxide no ordered superlattice appears. This is similar to the case of the benzene/Rh(111) system, where the coadsorption of carbon monoxide with benzene also gives rise to two separate ordered LEED patterns,[7] labeled $\begin{pmatrix} 3 & 1 \\ 1 & 3 \end{pmatrix}$ or c(2$\sqrt{3}$x4)rect for the first pattern and (3x3) for the second pattern. Both of these benzene/Rh(111) structures have been studied using LEED intensity analysis.[1,2] On Rh(111) another (somewhat less well- ordered) superlattice pattern has been observed in the absence of carbon monoxide. This carbon monoxide free structure, labeled $\begin{pmatrix} 3 & 3 \\ 2 & 2 \end{pmatrix}$ or (2$\sqrt{3}$x3)rect, has not been studied using LEED intensity analysis. However, the observed glide-plane symmetry implies bridge site adsorption for the benzene molecules in

this structure.[7] Carbon monoxide coadsorption shifts the benzene molecules to hollow sites on Rh(111).

Closer examination of the diffraction patterns of the previously reported ordered structures of benzene on Pt(111) revealed the existence of glide-planes along the [11$\bar{2}$] direction of both ordered structures.[8] This additional element greatly reduces the number of possible structural models. In particular the unit cells of both observed structures must contain pairs of symmetry-related molecules for each coadsorbed species.

When the ordered structures of benzene on Pt(111) were first observed, a model was proposed involving benzene molecules packed together with the carbon ring tilted relative to the surface, and no carbon monoxide coadsorption. This model was based on work function changes observed at large benzene exposures, and a large surface concentration of carbon, as determined by Auger spectroscopy.[3]

These observations can be re-interpreted now that the influence of carbon monoxide coadsorption on benzene ordering is understood. We have found more recently that a benzene exposure of ~2 L saturates the Pt(111) surface. This is consistent with the observation of Tsai, et al.[4] that a saturation coverage of deuterated benzene can be mostly displaced from Pt(111) by a ~2 L exposure of unlabeled benzene. The effect of prolonged exposure to benzene vapor was to allow carbon monoxide, a background gas in

most ultra-high vacuum systems, to coadsorb on the Pt(111) surface (carbon monoxide will displace benzene from Pt(111)[7]). Charge transfer between the carbon monoxide molecular orbitals and the metal surface can account for the observed work function changes.[9] This explanation is consistent with the observed downward shift in the carbon monoxide stretch frequency observed in HREELS.[7]

It was not possible to reproduce the large surface carbon concentrations reported by Stair, et. al.[3], during formation of the benzene ordered structures on Pt(111). Measurements by Tsai et. al.,[4] Davis et. al.,[10] and by us are consistent with much lower carbon coverages, of ~.9 - 1.0 carbon atoms per surface platinum atom, which is appropriate for flat-lying benzene molecules.

In this paper we report on the surface structure of the ordered Pt(111)-(2√3x4)rect-$2C_6H_6$+nCO superlattice, where the number n of carbon monoxide molecules per unit cell is probably, but not certainly, four.

2. LEED EXPERIMENT

The LEED experiments were conducted in a standard stainless-steel, ion-pumped ultra-high vacuum system, which was equiped with a four-grid LEED optics. An off-axis electron gun was used, together with the LEED retarding field energy analyzer, for Auger measurements. An ion bombardment gun was

used for crystal cleaning and a quadrupole mass spectrometer for residual gas analysis.

A platinum (111) single crystal, prepared by standard metallographic techniques, was mounted on a sample manipulator capable of independent azimuthal and polar angle rotation. The platinum crystal was spot-welded to a pair of tantalum foil strips supported by the sample manipulator. The crystal could be heated above 1400 K by passing a current through the supports, or cooled below 140 K by conduction from a pair of liquid nitrogen reservoirs attached to the supports. The crystal temperature was monitored by a .005" chromel-alumel thermocouple spot-welded to the edge of the platinum crystal.

The platinum crystal was prepared for the LEED experiments by sputter-cleaning at 1000 K with 500 eV argon ions, followed by annealing at 1300 K. Residual carbon was removed by heating the crystal to 1000 K in the presence of 2×10^{-7} torr of oxygen. The trace impurities dissolved in the platinum crystal were sulfur, silicon, calcium, and phosphorus. Hydrogen, oxygen, and carbon-containing molecules were deposited on the surface of the crystal from residual gases in the vacuum chamber. The cleaning procedure described above reduced the surface concentration of all these impurities below the Auger detection threshold, which is ~1%.

The vacuum system was enclosed in a set of Helmholtz coils, which were used to neutralize the magnetic fields in the vicinity of the crystal and LEED optics during LEED data collection. The LEED data were collected with a high-sensitivity vidicon camera and recorded on video tape, with the

electron gun under computer control. The video tape was played back into a full-frame, real-time video digitizer interfaced to an LSI-11/23 laboratory computer. This system, developed in our laboratory, was then used to generate LEED intensity-voltage (I-V) curves from the stored diffraction images.[11]

Spectroscopic-grade benzene was introduced into a glass and stainless-steel gas manifold. The benzene sample was degassed by freezing the sample, pumping over it and then thawing the sample. This procedure was repeated several times. Benzene was introduced into the UHV chamber through a leak valve and a stainless-steel doser tube 3 mm in outside diameter. (The vapor pressure of benzene at room temperature is ~100 torr.) The end of the doser tube was located ~5 cm away from the crystal so as not to block the view of the LEED screen.

The LEED data of the ordered benzene overlayers were collected before the significance of carbon monoxide coadsorption was understood.[7] The surface was prepared by flashing the crystal above 500 K to desorb any hydrogen or carbon monoxide adsorbed from the background gases (the system base pressure was $\sim 5 \times 10^{-10}$ torr during this work). The crystal was then exposed to benzene from the doser tube at 1×10^{-6} torr (uncorrected ion-gauge reading) for 600 seconds to form the (2√3x4)rect superlattice, or for 1200 seconds to form the (2√3x5)rect superlattice. After such a large exposure it took ~40 minutes for the system pressure to pump down to $\sim 10^{-9}$ torr. The crystal was then cooled to 140 K before recording the LEED data.

Measuring LEED I-V curves for the ordered structures of benzene on platinum is complicated by the dense array of spots from the large surface

unit cell. The LEED patterns of three rotated domains of the rectangular unit cell are superimposed in these structures. For the (2√3x4)rect structure adjacent diffraction beams may be separated by only 1/8 of the substrate beam spacing, and for the (2√3x5)rect structure the minimum separation is 1/20 of the substrate beam spacing. Because of the large number of diffraction beams, the fraction of the total diffracted intensity in each individual beam is reduced. Also, organic overlayers are often less well ordered than clean or reconstructed metal and semiconductor surfaces, resulting in broader, lower contrast diffraction beams. Although LEED data were recorded for both ordered structures, we have only been able to generate I-V curves for the (2√3x4)rect data. The overlap of diffraction beams in the more dense LEED pattern of the (2√3x5) structure has so far prevented successful generation of reliable I-V curves for this structure.

LEED data were recorded at both room temperature and 140 K. It was not possible to obtain a sufficient range of I-V data from the room-temperature measurements because of the low contrast in the LEED patterns.
At 140 K thermal diffuse scattering is reduced and the contrast in the diffraction pattern is improved, resulting in a larger range of useful I-V data. The following discussion refers to the 140 K data.

LEED data were collected at normal incidence between 12 and 150 eV. The diffraction data were analyzed to produce I-V curves for 3 independent substrate diffraction beams and ten independent superlattice beams, labeled (1,0), (0,1), (1,1), (-3/8,1/4), (3/8,-1/4), (-1/2,1/2), (1/2,-1/2), (1,-1/2), (3/8,-3/4), (-1/8,-3/4), (1/4,-1), (-5/8,-1/4) and (-1,1/4). The cumulative energy range for all these beams is 978 eV. The I-V curves of symmetry-related beams were compared to confirm normal incidence, and I-V

curves from two independent experiments were compared to show reproducibility. The large number of independent I-V curves available at normal incidence provided a sufficient data base for the structure analysis calculations.

3. LEED THEORY

All theoretical methods which we have applied in this work have been described in conjunction with the structural determinations of benzene/Rh(111).[1] Only a summary is given here.

Within the Combined Space Method[12] we have used Renormalized Forward Scattering to stack layers. The substrate layer diffraction was calculated accurately with conventional methods.[12] The overlayer diffraction matrices were obtained with several approximate schemes, namely kinematic approximation, near-neighbor or full multiple scattering within the Reverse Scattering Perturbation scheme, Matrix Inversion within individual molecules, and Kinematic Sublayer Addition. Also, Beam Set Neglect was applied. During the course of the structural search, successively more accurate approximations were chosen. An initial search through a wide range of structures was performed with the kinematic approximation within the overlayer. A more refined search through promising structures was then carried out with higher-precision calculations, etc. The next section will detail this procedure. All these calculational schemes enabled us to efficiently handle the large (2√3x4)rect superlattice unit cell and the

many atoms it contains. This unit cell has an area 16 times that of a (1x1) unit cell, producing 16 times more beams than a (1x1) structure, and it contains 2x6 = 12 carbon atoms for benzene and up to 8 carbon and oxygen atoms for carbon monoxide.

Glide-plane symmetry allows calculational savings identical to those of other forms of symmetry (rotational and mirror symmetries). The only significant difference appears in the formalism. With non-glide-plane symmetries, one retains only the symmetrical combinations of wave functions; the antisymmetrical combinations are rejected since the incident beam does not couple to these when the incidence direction is parallel to the axis or plane of symmetry. With glide-plane symmetry, either the symmetrical or the antisymmetrical combination comes into play, depending on which diffracted beams are considered. This choice also depends on which layer is diffracting, since typically only the overlayer has structural glide-plane symmetry while underlying substrate layers do not. Futher details can be found in reference 13.

The non-structural parameters in our LEED calculations for the substrate were selected as described in a previous LEED study of clean and carbon monoxide-covered Pt(111).[14] Phase shifts up to $\ell_{max} = 4$ were used.

Also, as before[1,2], five R-factors and their average were applied to compare theory and experiment.[15]

4. STRUCTURES TESTED

Our structural search for Pt(111)-(2√3x4)rect-2C_6H_6+xCO was very similar to our analyses for Rh(111)-$\begin{pmatrix} 3 & 1 \\ 1 & 3 \end{pmatrix}$-$C_6H_6$+CO and Rh(111)-(3x3)-$C_6H_6$+2CO. The likely structural possibilities are severely restricted by the unit cell size, the presence of a glide-plane symmetry, the thermal desorption data and the HREELS data, as well as approximate Van der Waals sizes for benzene and carbon monoxide. The benzene molecules were assumed to lie parallel to the Pt(111) surface, centered over bridge sites (although we also tested other high-symmetry sites). The carbon monoxide molecules were taken to stand perpendicularly to the surface, over bridge sites or hollow sites. Table 1 shows the chronological sequence of structures which we have tested, together with the calculational methods employed, while Figure 2 illustrates the geometrical relationships. The number of carbon monoxide molecules per unit cell is probably four, judging by the available space in the unit cell, although any benzene ring expansion (which we did find, see next Section) makes the fit rather tight. The HREELS[7] data exhibit two or possibly three C-O stretch frequencies, which might be attributed to bridge- and hollow-site bonding and possibly also top-site bonding. However, with four carbon monoxide molecules per unit cell, Van der Waals size considerations make any occupation of non-bridge sites unrealistic. We have also tried two carbon monoxide molecules in hollow sites per unit cell, and, since bridge-site-like metal-carbon spacings were systematically favored in the comparison with measured LEED intensities, hollow- and top-sites were not further explored.

Two high-symmetry azimuthal (Φ) orientations of the benzene molecules were investigated (Table 1 and Figure 2a, b). But in the bridge sites only the $\Phi = 0°$ option is probable, based on Van der Waals packing considerations; this is corroborated by the R-factor comparisons. We have studied distortions of the carbon rings: due to the strong benzene-metal bonding and weak molecule-molecule interaction, it is likely that any distortion is consistent with the local bonding symmetry, which in a bridge site consists of two perpendicular mirror planes (neglecting the effect of the second metal layer). We have therefore tried the cyclohexane boat shape (and not the chair shape) as an out-of-plane distortion of benzene, where two diametrically opposite carbon atoms move simultaneously above or below the plane of the remaining four ring atoms. In-plane distortions of the same two-dimensional symmetry have two equal-length bonds opposite each other, leaving the other four C-C bonds of common length. We have independently varied the radial distance from the ring center for the two end carbon atoms (those on a mirror plane) and for the four side carbon atoms (those off the mirror planes), and the C-C bond lengths by changing the azimuthal distortion angle β (see Table 1 and Figure 2d). We have also tried a Kekulé-type distortion (alternating long and short bonds around the carbon ring), which, however, did not prove promising.

Altogether, we tested approximately 750 distinct structures. Representative R-factor plots (Figure 3) illustrate the sensitivity to various structural parameters.

5. RESULTS

By minimizing the R-factors, we obtain the optimized structure for Pt(111)-(2√3x4)rect-2C_6H_6+4CO shown in Figure 4. Benzene molecules occupy bridge sites with the $\Phi = 0°$ azimuthal orientation of the carbon ring, the orientation favored from the Van der Waals geometry (Figure 2). Two possibilities exist for the second and deeper metal layer registry, labeled d'ABC+d"ABC and d"ABC+d'ABC in Table 1: the former choice was slightly favored by a five-R-factor average of 0.316 vs 0.327 under the conditions shown in Table 1. This is too small a difference to determine the registry. We have not attempted to resolve this question, given the very minor structural difference that it represents. In any case, both registries may co-exist.

Out-of-plane distortions in the "boat" shape drastically worsened the average R-factor, from about 0.28 to about 0.38 for both up and down distortions (Table 1). We estimate such buckling displacements perpendicular to the surface to be less than ~0.05Å. A strong, but nearly six-fold symmetrical in-plane distortion is found in the carbon rings: radii of 1.79±0.15Å for the two end carbons and radii of 1.72±0.15Å for the four side atoms, with an azimuthal distortion of $\beta = 1.5 \pm 2.5°$; this translates to two shorter C-C bonds of length 1.65±0.15Å and four longer C-C bonds of length 1.76±0.15Å. The shorter bonds lie over single platinum atoms, while the longer bonds form bridges over pairs of platinum atoms.

The carbon ring is found at a height of 2.10±0.10Å above the Pt(111) surface. As a result, the six platinum-carbon bond lengths are equal to 2.25Å within ±0.10Å. Two separate values might be expected, given the local bonding symmetry at a bridge site, but the bond lengths differ in our results by rather less than the uncertainty of 0.10Å. This fact independently supports a planar carbon ring, since nearly equal metal-carbon bond lengths are implied, which is intuitively appealing.

There is less certainty about the number and location of carbon monoxide molecules. Average R-factors of 0.315 and 0.321 were obtained for two carbon monoxide molecules per unit cell in bridge and in hollow sites, respectively. The nearest comparable structure with four CO molecules, all in bridge sites, yielded a similar R-factor of 0.316. However, a metal-carbon layer spacing for the carbon monoxide molecules of 1.45±0.10Å was systematically found for most of the structures shown in Table 1, including the hollow-site arrangement. This spacing is most consistent with bridge sites, yielding metal-carbon bond lengths of 1.99±0.07Å. The C-O bond length was optimized at 1.15±0.10Å.

Thermal desorption results in reference 7 suggest four carbon monoxide molecules per unit cell. Based on Van der Waals sizes, four carbon monoxide molecules will fit in the unit cell for our optimum geometry (Figure 4).

Our best structure, with four carbon monoxide molecules in bridge sites, has a five-R-factor average of about 0.28, and corresponding Zanazzi-Jona and Pendry R-factors of about 0.42 and 0.54. These R-factor values may be compared, respectively, with 0.31, 0.40 and 0.66 for Rh(111)-$\begin{pmatrix} 3 & 1 \\ 1 & 3 \end{pmatrix}$-$C_6H_6$+CO and with 0.21, 0.24 and 0.41 for Rh(111)-(3x3)-C_6H_6+2CO. The optimized muffin-tin zero level is found at 14±1 eV below the vacuum zero energy for the structure on Pt(111).

6. DISCUSSION AND CONCLUSIONS

Carbon monoxide can cause two forms of long-range order for benzene on Pt(111), which otherwise is disordered at all benzene coverages.[5,6] In the (2√3x4)rect structure, benzene is centered on bridge sites with a large carbon ring expansion and no detectable out-of-plane buckling. The carbon monoxide molecules are probably located in bridge sites as well and may number four per unit cell, i.e., two per benzene. The (2√3x5)rect structure of benzene and carbon monoxide has not been analyzed with LEED intensities. But, it presents very close similarities to the (2√3x4)rect structure: glide-plane symmetry in the LEED pattern, nearly identical high-resolution electron energy loss spectra, but with thermal desorption spectra indicating more adsorbed carbon monoxide. Therefore, we expect its detailed structure to be similar to that of the (2√3x4)rect arrangement, with possibly six carbon monoxide molecules per unit cell, i.e., three per benzene.

We must point out one possible discrepancy between our final model for the (2√3x4)rect arrangement and the corresponding HREELS data: these show three C-O stretch frequencies, indicating possibly three carbon monoxide bonding sites. Our model contains at most two inequivalent types of carbon monoxide molecules. The preferred bridge sites for these two molecules are

not quite equivalent in terms of their neighborhood. One carbon monoxide molecule is in close contact with three benzenes and the second carbon monoxide molecule, while this second molecule touches only one benzene and the first carbon monoxide. Whether this difference is large enough to cause two of the three C-O stretch frequencies is not clear. The third frequency is probably due to carbon monoxide molecules in defect sites or outside the ordered benzene+carbon monoxide regions. This vibrational mode was not observed in the HREEL spectra when the (2√3x4)rect structure was formed at room temperature. Only after cooling to nitrogen temperature did this third mode appear in the HREEL spectra.[7] There was no apparent change in the long-range order of the LEED pattern on cooling.

Table 2 compares the present structural result with the other benzene structures on Rh(111) surfaces, as well as with gas-phase benzene, benzene in organo-metallic complexes, acetylene and ethylene parallel-bonded on Pt(111) and ethylidyne (CCH_3) bonded on Rh and Pt(111). Some theoretical results obtained with the Extended Hückel molecular orbital method are included for benzene on Rh(111).

As discussed in Reference 1, the coadsorption of benzene and carbon monoxide generates new ordering arrangements not present with the separate adsorption of benzene alone or carbon monoxide alone. The adsorption sites themselves can be modified by coadsorption. The tendency is for benzene to move from bridge sites to hollow sites due to carbon monoxide coadsorption on Rh(111) (the same hcp-type hollow sites in both structures on Rh(111)). The carbon monoxide molecules tend towards higher-coordination sites due to coadsorption of benzene, especially on Rh(111). A charge transfer from benzene via the substrate to carbon monoxide may explain this behavior. C-O bond elongation, suggested especially by the Rh(111)-$\begin{pmatrix} 3 & 1 \\ 1 & 3 \end{pmatrix}$-$C_6H_6$+CO struc-

ture, is consistent with this picture. Less C-O elongation for Rh(111)-(3x3)-C_6H_6+2CO and Pt(111)-(2√3x4)rect-2C_6H_6+4CO might be explained by the sharing of benzene-donated charge among more carbon monoxide molecules (this is also consistent with a slight increase of the C-O stretch frequency which occurs at the same time). It is not clear at this point why the Rh-C bond length for CO appears to differ considerably between the $\binom{31}{13}$ and the (3x3) structures: 2.16±0.04Å and 2.02±0.07Å, respectively.

The benzene adsorption site varies as is shown in Table 2. In the absence of carbon monoxide, benzene is probably located in bridge sites both on Rh(111)[1] and on Pt(111).[8] Our results indicate that the carbon ring can distort in a way compatible with the site symmetry, i.e. with $C_{3v}(\sigma_d)$ symmetry over hollow sites and C_{2v} symmetry over bridge sites (or C_s symmetry if deeper metal layers are taken into account). The main effect of adsorption is a carbon ring expansion, such that the mean ring radius is 1.58±0.15Å, 1.51±0.15Å and 1.72±0.15Å, respectively for Rh(111)+$\binom{31}{13}$-C_6H+CO, Rh(111)-(3x3)-C_6H_6+2CO and Pt(111)-(2√3x4)rect-2C_6H_6+4CO. In the $\binom{31}{13}$ structure we find also a strong variation between C-C bonds (three short bonds and three long bonds), which is not apparent in the two other structures (we must keep in mind the relatively large error bars of ±0.15Å on these distances). As mentioned in more detail in Reference 1, similar but weaker distortions are found in organometallic complexes. New results[9] are now available for two complexes containing benzene symmetrically placed against a metal triangle, $Ru_6C(CO)_{11}(C_6H_6)_2$ and $Os_3(CO)_9(C_6H_6)$. As Table 2 shows, these exhibit the Kekulé-type distortion of our $\binom{31}{13}$ structure. Although it is less strong, this distortion also features a carbon ring expansion to a radius of 1.44±0.02Å. Similar expansions are found with near edge x-ray absorption fine

structure (NEXAFS) measurements for acetylene and ethylene parallel-bonded to the Pt(111) surface.[17] The Extended-Hückel results[18] also predict a ring expansion, to about 1.52Å, and a possible Kekulé-type distortion with C-C bond lengths of up to 1.50 and 1.64Å, respectively, for the short and long bonds. Ethylidyne (CCH_3) species have C-C bonds perpendicular to the surface. Although these bonds are not in direct contact with the metal, unlike the case of benzene, they provide a valuable reference point for comparison of C-C bond lengths: see Table 2.

No evidence for benzene ring expansion was found in NEXAFS studies of disordered benzene adsorbed on Pt(111) (without carbon monoxide); the carbon-carbon bond length was found to be within ±0.02Å of the gas-phase value of 1.40Å.[6] This does not necessarily contradict our LEED results. For benzene adsorbed on Rh(111) the distortions of the benzene carbon ring vary significantly from site to site (Table 2). Therefore, our LEED results for benzene on bridge sites coadsorbed with carbon monoxide may be consistent with the NEXAFS results for disordered benzene adsorbed in undetermined sites.

Recent measurements with angle-resolved ultraviolet photoelectron spectroscopy have been made[19] for benzene with and without carbon monoxide on Rh(111); the case with carbon monoxide had the (3x3) pattern, while the carbon monoxide-free case is claimed to have the $\begin{pmatrix} 3 & 1 \\ 1 & 3 \end{pmatrix}$ pattern (our results suggest that this pattern is due to some coadsorbed carbon monoxide). These data appear to indicate that no deviation from six-fold symmetry occurs, i. e. that all C-C bonds in the carbon ring are equally long. Our results may be consistent with these observations. In the (3x3) case, our Kekulé-type

distortion is possibly slight, while in the carbon monoxide-free (bridge site) case, our analogous (bridge site) result on Pt(111) shows only small variations between C-C bond lengths. Photoemission may be insensitive to such small deviations from 6-fold symmetry.

The HREELS data[7] are not inconsistent with our findings. They show large shifts in benzene vibration-mode frequencies between the gas phase and the adsorbed state. However, in the present state of the art the HREELS data cannot be interpreted in terms of presence or absence of C_6-ring distortions.

Finally, our results suggest a connection with the catalytic reactivity of Rh and Pt for benzene reactions. The platinum (111) crystal face is an excellent catalyst for the production of benzene from n-hexane or n-heptane (dehydrocyclization). This is an important reaction that is used in petroleum refining to produce high octane gasoline. The Rh(111) crystal face, however, cannot carry out this catalytic reaction due to the rapid fragmentation of benzene on the metal surface (hydrogenolysis) under the reaction conditions. Perhaps the large Kekule distortion of the adsorbed aromatic molecule observed in one of our structures on rhodium is indicative of preferential C-C bond breaking to produce CH and C_2H fragments, which occurs as the temperature is increased.[22] Benzene chemisorbed on the Pt(111) crystal face is less asymmetrically distorted, exhibiting a more uniform expansion of the ring. This structure may suggest a benzene intermediate on the metal surface that can desorb intact at the higher temperatures and pressures of the catalytic reaction. Future studies will test further the possible correlation between molecular surface structures and catalytic reaction intermediates.

ACKNOWLEDGEMENTS

We thank C. Minot, M. Simonetta, A. Gavezzotti and E. Garfunkel for fruitful discussions, made possible by a NATO US-France exchange grant and an NSF US-Italy exchange grant.

This work was supported by the Director, Office of Energy Research, Office of Basic Energy Sciences, Materials Science Division, of the U. S. Department of Energy under Contract Number DE-AC03-76SF00098. Supercomputer time was also provided by the Office of Energy Research of the Department of Energy.

REFERENCES

1. M.A. Van Hove, R. F. Lin, and G. A. Somorjai; J. Amer. Chem. Soc, in press.

2. R.F. Lin, G.S. Blackman, M.A. Van Hove, and G.A. Somorjai, to be published.

3. J.L. Gland and G.A. Somorjai, Surf. Sci. 38, 157 (1973);
   P.C. Stair and G.A. Somorjai, J. Chem. Phys. 67, 4361 (1977).

4. M.C. Tsai and E.L. Muetterties, J. Amer. Chem. Soc. 104, 2534 (1982)

5. S. Lehwald, H. Ibach, and J.E. Demuth, Surf. Sci. 78, 577 (1978).

6. J.A. Horsley, J. Stöhr, A.P. Hitchcock, D.C. Newbury, A.L. Johnson, and F. Sette, J. Chem. Phys. 83, 6099 (85).

7. C.M. Mate and G.A. Somorjai, Surf. Sci. 160, 542 (1985).

8. R.F. Lin, R.J. Koestner, M.A. Van Hove, and G.A. Somorjai, Surf. Sci. 137, 161 (1983).

9. E.L. Garfunkel, M.H. Farias, G.A. Somorjai, J Amer Chem Soc, 107, 349 (1985)

10. S.M. Davis, B.E. Gordon, M. Press, G.A. Somorjai, JVST 19, 231 (1981)

11. D.F. Ogletree, J.E. Katz, G.A. Somorjai, Rev. Sci. Inst., in press.

12. M.A. Van Hove and S.Y. Tong, "Surface Crystallography by LEED", Springer-Verlag (Heidelberg) (1979).

13. M.A. Van Hove, W.H. Weinberg and C-M. Chan, "Low-Energy Electron Diffraction: Experiment, Theory and Structural Determination", Springer-Verlag (Heidelberg), in press.

14. D.F. Ogletree, M.A. Van Hove, and G.A. Somorjai, Surf. Sci. 173, 351 (1986).

15. R.J. Koestner, M.A. Van Hove and G.A. Somorjai, Surf. Sci. 107, 439 (1981).

16. M.P. Gomez-Sal, B.F.G. Johnson, T. Lewis, P.R. Raithby, and A.H. Wright, J. Chem. Soc., Chem. Commun. 1985, 1682.

17. J. Stöhr, F. Sette and A. L. Johnson, Phys. Rev. Letters 53, 1684 (1984).

18. C. Minot, E.L. Garfunkel, A. Gavezzotti, and M. Simonetta, to be published.

19. J.U. Mack, E. Bertel, and F.P. Netzer, Sci. 159, 265 (1985); and private communications.

20. L.L. Kesmodel, L.H. Dubois, and G.A. Somorjai, J Chem Phys 70, 2180 (1979).

21. R.J. Koestner, M.A. Van Hove and G.A. Somorjai, Surf. Sci 121, 321 (1982).

22. P.-K. Wang, C.P. Slichter and J.H. Sinfelt, J. Phys. Chem. 89, 3606 (1985).

23. J.A. Horsley, J. Stöhr and R.J. Koestner, J. Chem. Phys. 83, 3146 (1985).

24. Surface Crystallography Information Service, J.B. Pendry and M.A. Van Hove, to be published.

TABLE 1 STRUCTURES EXAMINED

Composition	Site[a] C_6H_6	Site[a] CO	$\vartheta(°)$[b]	$d_{\perp M-C6}(Å)$[c]	$d_{\perp M-CO}(Å)$[g]	$d_{C-O}(Å)$[h]	Buckling	Ring Distortion[e] r(Å)	Ring Distortion[e] β(°)	Method[f]
$2C_6H_6$	2xaABC	-	0, 30	1.2(.1)2.1	-	-	None	1.397	0	BSN + partial RSP
$2C_6H_6$	2xbABC	-	0, 30	1.5(.1)2.4	-	-	None	1.397	0	BSN + partial RSP
$2C_6H_6$	2xcABC	-	0, 30	1.5(.1)2.4	-	-	None	1.397	0	BSN + partial RSP
$2C_6H_6$	2xdABC	-	0, 30	1.5(.1)2.4	-	-	None	1.397	0	BSN + partial RSP
$2C_6H_6$	d'ABC+d"ABC	-	0, 30	1.5(.1)2.4	-	-	None	1.44 Kekule:	±4	BSN + partial RSP
$2C_6H_6$	d'ABC+d"ABC	-	0, 30	1.5(.1)2.4	-	-	None	1.44	±4	BSN + partial RSP
$2C_6H_6$+4CO	d'ABC+d"ABC[i]	2xd'ABC[i]+ 2xbABC	0, 30	1.9(.1)2.4	1.3(.1)1.6 1.27(.1)1.57	1.15	None	1.397	0	Kinematic
$2C_6H_6$+4CO	d"ABC+d'ABC[i]	2xd"ABC[i]+ 2xcABC	0, 30	1.9(.1)2.4	1.3(.1)1.6 1.27(.1)1.57	1.15	None	1.397	0	Kinematic
$2C_6H_6$+4CO	d'ABC+d"ABC	4xd'ABC	30	1.9(.1)2.4	1.3(.1)1.6	1.15	boat up 0.36Å	1.397	0	Kinematic
$2C_6H_6$+4CO	d'ABC+d"ABC	4xd'ABC	30	1.54(.1)2.04	1.3(.1)1.6	1.15	boat down 0.36Å	1.397	0	Kinematic
$2C_6H_6$+4CO	d"ABC+d'ABC	4xd"ABC	30	1.9(.1)2.4	1.3(.1)1.6	1.15	boat up 0.36Å	1.397	0	Kinematic
$2C_6H_6$+4CO	d"ABC+d'ABC	4xd"ABC	30	1.54(.1)2.04	1.3(.1)1.6	1.15	boat down 0.36Å	1.397	0	Kinematic
$2C_6H_6$+4CO	d'ABC+d"ABC	4xd'ABC	0	1.4(.1)1.9	1.3(.1)1.6	1.15	boat up 0.36Å	1.397	0	Kinematic

TABLE 1 cond't

Composition	Site[a] C_6H_6	Site[a] CO	$\Phi(°)$[b]	$d_{\perp M-C6}(Å)$[c]	$d_{\perp M-CO}(Å)$[g]	$d_{C-O}(Å)$[h]	Buckling	Ring Distortion[e] r(Å)	Ring Distortion[e] β(°)	Method[f]
$2C_6H_6+2CO$	d'ABC+d"ABC	2xd'ABC	30	1.9(.1)2.4	1.3(.1)1.6	1.15	None	1.397	0	Kinematic
$2C_6H_6+2CO$	d'ABC+d"ABC	2xbABC	30	1.9(.1)2.4	1.3(.1)1.6	1.15	None	1.397	0	Kinematic
$2C_6H_6+4CO$	d'ABC+d"ABC	4xd'ABC	30	2.05(.05)2.30	1.55	1.15	None	1.2(.13)1.59	0	Kinematic
$2C_6H_6+4CO$	d'ABC+d"ABC	4xd'ABC	30	2.05(.05)2.30	1.55	1.15	None	1.59	-2.5(5)7.5	BSN+KSLA +MINV
$2C_6H_6+4CO$	d'ABC+d"ABC	4xd'ABC	30	2.05(.05)2.30	1.35(.1)1.65	1.15	None	1.59(.13)1.85	0	BSN+KSLA +MINV
$2C_6H_6+4CO$	d'ABC+d"ABC	4xd'ABC	30	2.05(.05)2.30	1.35(.1)1.65	1.15	None	1.72	-2.5,1.5,2.5	BSN+KSLA +MINV
$2C_6H_6+4CO$	d'ABC+d"ABC	4xd'ABC	30	2.05(.05)2.30	1.35(.1)1.65	1.15	Boat up/ down ±0.36Å	1.72	-1.5	BSN+KSLA +MINV
$2C_6H_6+4CO$	d'ABC+d"ABC	4xd'ABC	30	2.05(.05)2.30	1.35(.1)1.65	1.15	None	$(r_t,r_e)^j$= (1.59,1.72), (1.85,1.72), (1.72,1.85), (1.72,1.59)	1.5	BSN+KSLA +MINV
$2C_6H_6+4CO$	d'ABC+d"ABC	4xd'ABC	30	2.05(.05)2.30	1.35(.1)1.65	1.15	None	$(1.79,1.72)^j$	-1,0,4.0	BSN+KSLA +MINV
$2C_6H_6+4CO$	d'ABC+d"ABC	4xd'ABC	30	2.05(.05)2.30	1.35(.1)1.65	1.15	None	$(1.79,1.72)^j$	1.5	BSN+KSLA +MINV

NOTES TO TABLE 1

a. aABC = C_6H_6 centered on top site, bABC = hcp-hollow site, cABC = fcc-hollow site, dABC, d'ABC,d"ABC = 3 differently oriented bridge sites (see figure 2c).

b. C_6H_6 azimuthal orientation (see figure 2a & b).

c. Smallest layer spacing between atom nuclei and C_6 nuclei; notation $d_1(\Delta d)d_2$ implies values ranging from d_1 to d_2 in steps of Δd.

d. Out-of-plane distortion of C_6 ring, if any; "boat" is cyclohexane C_6 structure in boat arrangement, with tips tilted up or down by indicated amount with respect to plane of other four carbon atoms.

e. Non-Kekule distortions have C_{2v} symmetry of C_6 ring, characterized by r and β (see figure 2d), notation r_1/r_2 indicates radii r_1 for 2 end atoms of C_6 ring and radii r_2 for 4 side atoms of C_6 ring; Kekule distortion has $C_{3V}(\sigma_d)$ symmetry, characterized by r and β (see figure 2e).

f. Calculational method: Kinematic = all-kinematic in overlayer; BSN = Beam Set Neglect; KSLA = Kinematic Sublayer Addition; partial RSP = Reverse Scattering Perturbation with near-neighbor multiple scatterings only; MINV = Matrix Inversion instead of RSP.

g. Smallest layer spacing between metal nuclei and C nuclei of CO.

h. C-O bond length (CO bond always ⊥ surface).

i. The difference between d'ABC+d"ABC and d"ABC+d'ABC for C_6H_6, and between d'ABC and d"ABC for CO, refers to a minor structural difference due to two possible choices of registry in second (and deeper) metal layers.

j. r_t and r_e are independent radii for terminal atoms (on mirror plane) and lateral atoms (off mirror planes), respectively.

TABLE 2. ADSORPTION GEOMETRIES OF BENZENE

SYSTEM	$d^{<}_{C-C}$ (Å)	$d^{>}_{C-C}$ (Å)	$d_{\perp M-C}$(Å)	d_{M-C}(Å)	Site
Rh(111)-c(2√3x4)rect-C_6H_6+CO[a]	1.33±0.15	1.81±0.15	2.25±0.05	2.35±0.05	hollow
Rh(111)-(3x3)-C_6H_6+2CO[b]	1.46±0.15	1.58±0.15	2.20±0.05	2.30±0.05	hollow
Rh(111)-(3x3)-C_6H_6 (theory)[c]	1.50	1.64	2.1	2.15	hollow
Pt(111)-(2√3x4)rect-2C_6H_6+4CO[d]	1.65±0.15	1.76±0.15	2.10±0.10	2.25±0.10	bridge
Pt(111)-C_6H_6 disordered[e]	1.40±0.02				
C_6H_6 on metal clusters[f]	1.39	1.48		2.27-2.32	hollow
C_6H_6 molecule	1.397				
Pt(111)-(2x2)-C_2H_3(ethylidyne)[g]	1.50±0.1		1.20±0.1	2.00±0.07	hollow
Rh(111)-(2x2)-C_2H_3(ethylidyne)[h]	1.45±0.10		1.31±0.1	2.03±0.07	hollow
Pt(111)-C_2H_3 (ethylidyne)[i]	1.49±0.02				
Pt(111)-C_2H_3 (ethylidyne)[j]	1.47±0.03				
C_2H_6 molecule	1.54				
Pt(111)-C_2H_4[k]	1.49±0.03				
C_2H_4 molecule	1.33				
Pt(111)-C_2H_2[k]	1.45±0.03				
C_2H_2 molecule	1.20				

a. Ref. 1; b. Ref. 2; c. Ref. 18: this theory slightly favors a bridge site over a hollow site in the absence of CO; d. Ref. 14; e. Ref. 6; f. Ref. 16; g. Ref 20; h. Ref. 21; i. Ref. 22; j. Ref. 23; k. Ref. 17.

TABLE 3. STRUCTURE RESULT INFORMAT OF SURFACE CRYSTALLOGRAPHY INFORMATION SERVICE (SCIS)

SURFACE: Substrate Face: Pt(111); Adsorbate C_6H_6,CO;
Surface Pattern: (-2,2/4,4)=(2√3x4)rect.

STRUCTURE: Bulk Structure: FCC Temp; 150K; Adsorbate State: Molecular; Coverage 1/8 (C_6H_6/Pt), 1/4 (CO/Pt).

REFERENCE UNIT CELL: a=11.09Å; b=9.602Å; A(a,b)=90°.

Layer	Atom	Atom Positions		Normal Layer Spacing
A1	O	0.375	0.0	0.0
A2	O	0.625	0.0	0.0
A3	O	0.0	0.5	0.0
A4	O	0.25	0.5	0.5
A5	C	0.9955	0.1791	0.0
A6	C	0.1344	0.0896	0.0
A7	C	0.1326	0.9063	0.0
A8	C	0.0045	0.8209	0.0
A9	C	0.8656	0.9104	0.0
A10	C	0.8674	0.0937	0.0
A11	C	0.6295	0.6791	0.0
A12	C	0.7576	0.5896	0.0
A13	C	0.7594	0.4063	0.0
A14	C	0.6205	0.3209	0.0
A15	C	0.4924	0.4104	0.0
A16	C	0.4906	0.5937	0.65
A17	C	0.375	0.0	0.0
A18	C	0.625	0.0	0.0
A19	C	0.0	0.5	0.0
A20	C	0.25	0.5	1.45
S1	Pt	0.1875	0.125	0.0
S2	Pt	0.4375	0.125	0.0
S3	Pt	0.6875	0.125	0.0
S4	Pt	0.9375	0.125	0.0
S5	Pt	0.0625	0.375	0.0
S6	Pt	0.3125	0.375	0.0
S7	Pt	0.5625	0.375	0.0
S8	Pt	0.8125	0.375	0.0
S9	Pt	0.1875	0.625	0.0
S10	Pt	0.4375	0.625	0.0
S11	Pt	0.6875	0.625	0.0
S12	Pt	0.9375	0.625	0.0
S13	Pt	0.0625	0.875	0.0
S14	Pt	0.3125	0.875	0.0
S15	Pt	0.5625	0.875	0.0
S16	Pt	0.8125	0.875	2.26

2D Symmetry: PG;
Thermal Vibrations: Debye Temp=300K with double amplitude for surface atoms;
R-factor: R_{VHT}=0.28, R_F=0.54, R_{ZJ}=0.42.

FIGURE CAPTIONS

Figure 1. LEED pattern (panel a) with beam labeling (panel b) and corresponding surface unit cell (panel c) for a (2√3x4)rect overlayer on Pt(111). The pattern is decomposed into three domains of different orientations, only one of which is shown in panel c. Open symbols in pattern mark spots which are extinguished at special angles of incidence, in particular, at normal incidence.

Figure 2. Panels a and b show the molecular packing with a (2√3x4)rect overlayer on Pt(111) with the help of Van der Waals contours, for two benzene orientations (Φ = 0° and 30°) and four CO molecules per unit cell. Glide planes are indicated by dashed lines. Panel c represents four "registries" of the (2√3x4)rect overlayer (with Φ = 30°). The benzenes are represented by rings of carbons and hydrogens. Note atoms in the second metal layer, represented by dots which distinguish the registries bABC and cABC. Panels d and e show benzene distortions with local symmetries consistent with a bridge site (d) and a hollow site (e).

Figure 3. R-factor contour plots for pairs of structural variables, relating the CO and C_6H_6 heights over the metal surface ($d_{\perp Pt-C_1}$ and $d_{\perp Pt-C_6}$ respectively) to benzene distortions given by r and β (see figure 2d). Constant are d_{C-O} = 1.15Å and Φ = 30°. Except in the panel marked "kinematic", the calculational method is BSN+KSLA+MINV (see table 1).

Figure 4. Optimal structure for Pt(111)-(2√3x4)rect-2C_6H_6+4CO, in side view at top and plan view at bottom. Van der Waals shapes are used. The CO molecules are shown shaded. The side view projects both benzene and CO along the direction of the bridge that a benzene makes across two adjacent metal atoms. The hydrogen positions are guessed.

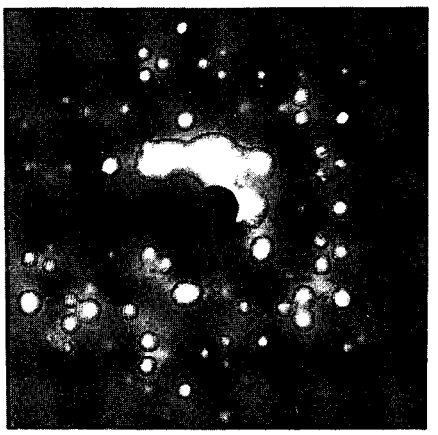

(a)

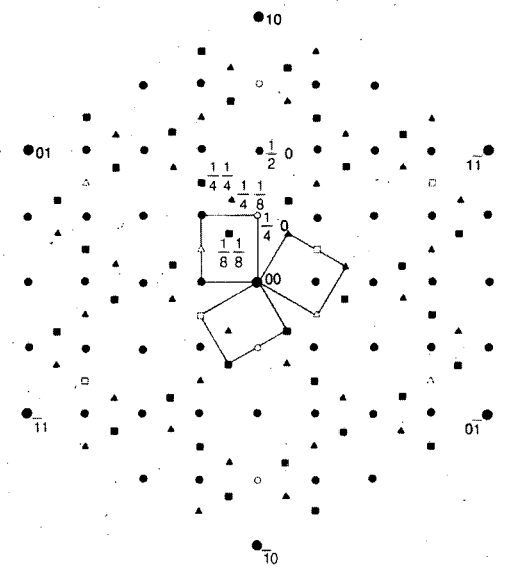

(b)

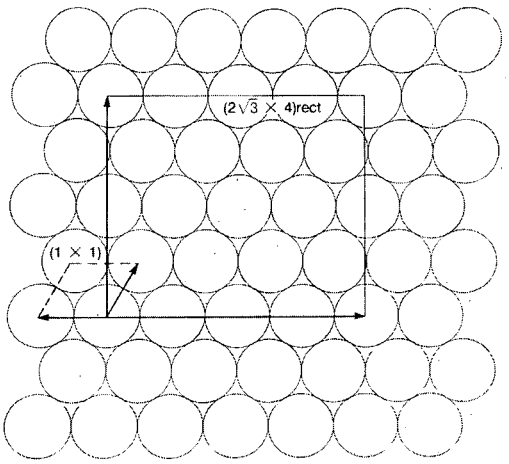

(c)

Figure 1

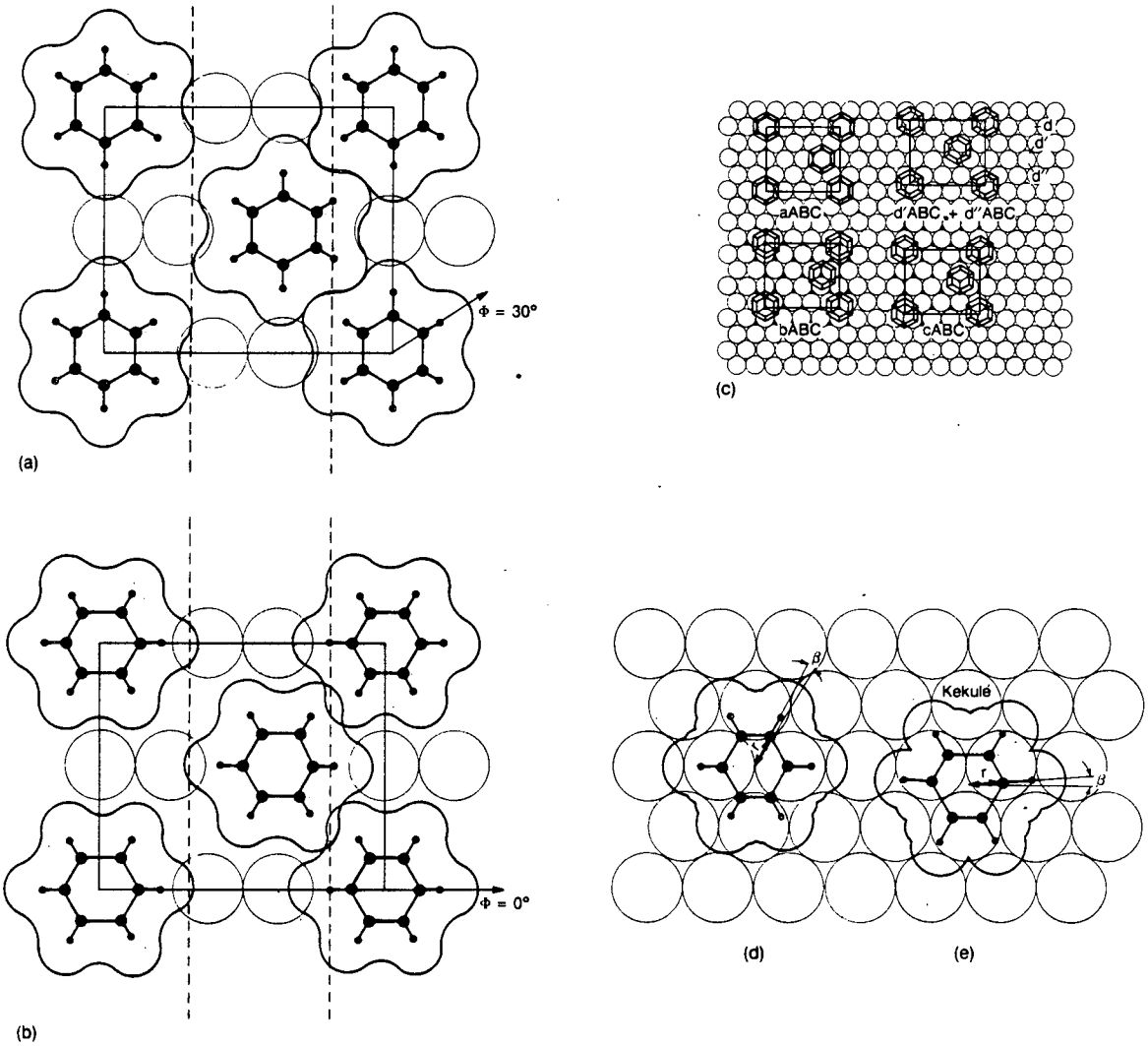

XBL 867-2544

Figure 2

Pt(111) – $(2\sqrt{3}\times4)$rect – $2C_6H_6$ + 4CO

R-factor contour plots

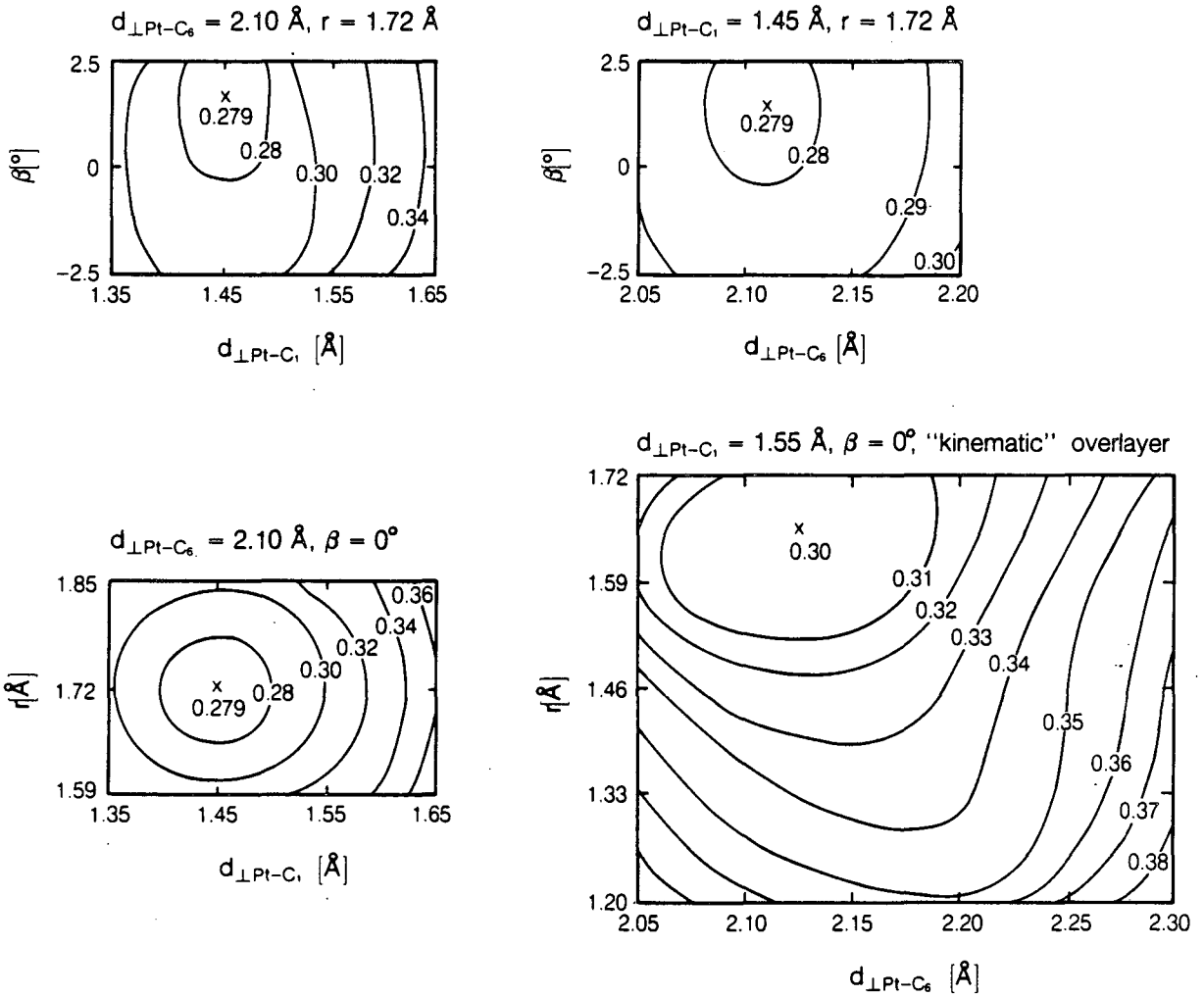

XBL 867-2542

Figure 3

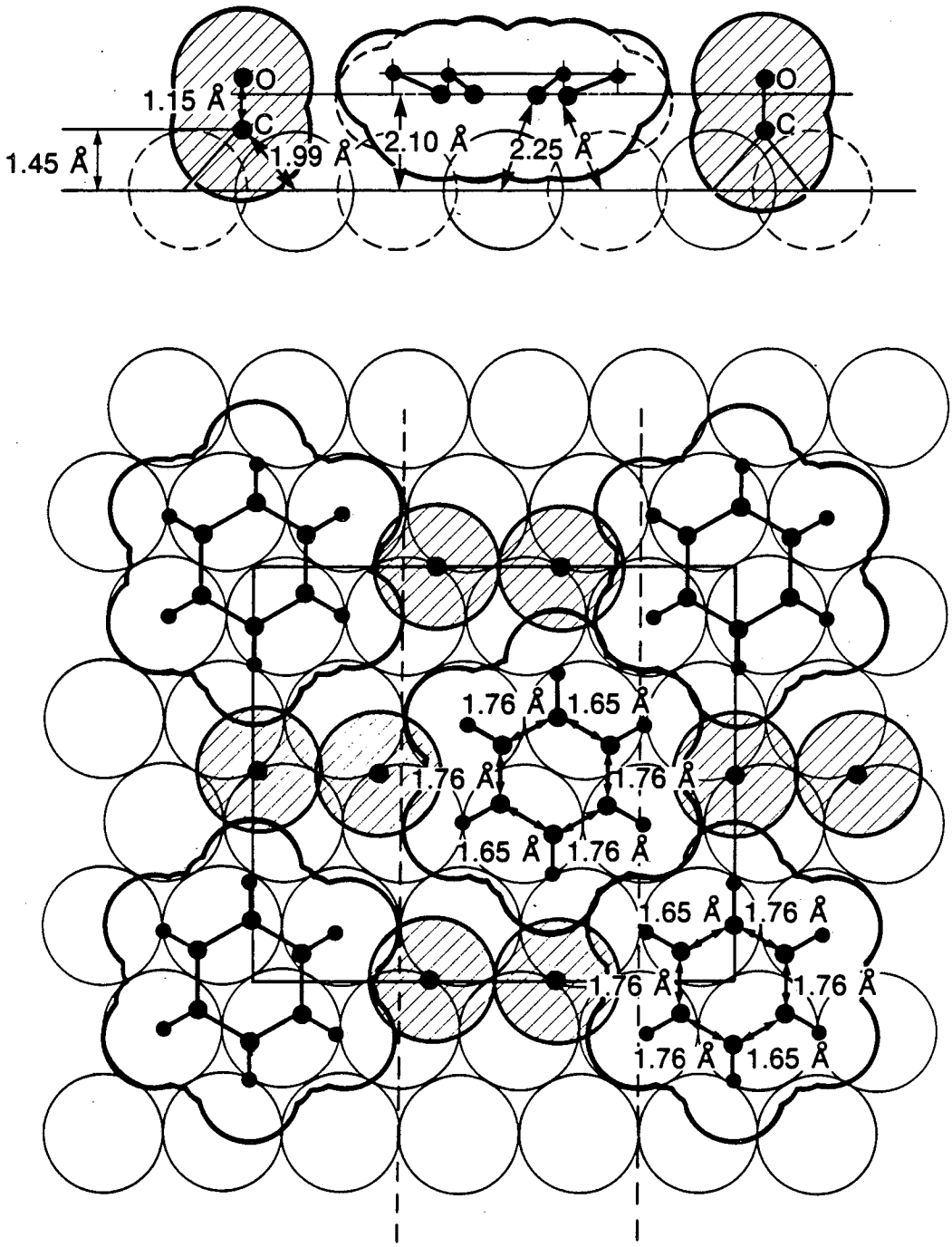

$Pt(111) - (2\sqrt{3}\times 4)rect - 2C_6H_6 + 4CO$

XBL 867-2543

Figure 4

LAWRENCE BERKELEY LABORATORY
TECHNICAL INFORMATION DEPARTMENT
UNIVERSITY OF CALIFORNIA
BERKELEY, CALIFORNIA 94720